RSC Advances

ROYAL SOCIETY OF CHEMISTRY

www.rsc.org/advances

RSC advances

ARTICLE

Antibacterial Properties And Cytocompatibility of Bio-based Nanostructure Carbon Aerogels Derived From Silver Nanoparticles Deposited Bacterial Cellulose†

Received 00th January 20xx,
Accepted 00th January 20xx

DOI: 10.1039/x0xx00000x

www.rsc.org/

Ning Yan, [‡a] Yabin Zhou, [‡b] Yudong Zheng, [a *] Shuang Qiao, [a] Qun Yu, [a] Zhongzheng Li, [a] and Haiyang Lu [a]

AgNP (silver nanoparticles)-deposited bio-based nanostructure carbon aerogels (denoted as p-BC/AgNP) with a three-dimensional (3D) porous network structure were fabricated by carbonizing the AgNP bacterial cellulose (denoted as BC/AgNP). The unique 3D nano-network structure gave the hydrophobic p-BC/AgNP good mechanical property and water reabsorption capacity. AgNP uniformly dispersed on the fibers, combining more firm with fibers after the carbonization process, and no massive release of Ag^+ emerged *in vitro* release test. As an antibacterial material, p-BC/AgNP has excellent antibacterial effect on *Escherichia coli (E. coli)* and *Staphylococcus aureus (S. aure)*, in which the inhibition rate was over 99 %. Moreover, p-BC/AgNP was good for cells attachment and normal proliferation, which was revealed by fluorescence microscope, field-emission scanning electron microscopy and MTT assay in Bel-7402 cell line. Because all of the above, p-BC/AgNP might be a desirable antibacterial material that could be used as a new kind of wound dressing, implants , drug release carrier, and other biomedical fields.

1. Introduction

With high porosity, large specific surface area and high electrical conductivity, carbon aerogel has been widely recognized as a promising material for capacitors, catalyst supports, adsorbents and gas sensors[1-4]. Traditional carbon aerogel is obtained from resorcinol formaldehyde organic aerogel pyrolysis under inert atmosphere, thus forming a highly crosslinked carbon network structure[5]. Recently, with the unique physical properties, such as low density, high porosity, high flexibility, high specific surface area and good electrical conductivity, the bio-based nanostructure carbon aerogels with three-dimensional network structure have attracted the attention of several researchers[6-8].

Bacterial cellulose (BC) is a polysaccharide synthesized from Acetobacter xylinus. Due to its high elastic modulus, biocompatibility, good water holding capacity, ultrafine three-dimensional network structure, low cost and easy accessibility, BC has been a promising biopolymer widely used in paper and food industries, sewage purification, acoustics, optics and medical fields[9-11]. To improve the antibacterial properties of BC in medical fields, BC is combined with different materials, such as Ag[12], chitosan[13], ZnO[14], TiO_2[15], montmorillonite (MMT)[16] and other antibacterial materials[17], in which Ag/NPs are one of the most widely used antimicrobial materials. However, the aggregation tendency of AgNPs (Ag nano-particles) in synthesis, the weak bonding between the fibers and the AgNPs, as well as the massive release behavior of AgNPs in a short time, may all cause cell toxicity and even more serious tissue reaction. Meanwhile, the water absorption capacity of BC is difficult to restore after dehydration, so the release capacity of AgNPs is limited and the antibacterial properties will be reduced. Some researchers have proposed several methods to solve these problems, as Table 1 showed. But they always tend to solve one of the problems by changing the synthetic methods or raw materials.

Table 1 Different improved methods by previous researchers

Raw Materials	Synthetic Methods	Source
Vegetable cellulose, Silver nanoparticles	UV radiation	18
Bacterial cellulose, Silver nanoparticles	$NaBH_4$ reduction	19
Bacterial cellulose, Silver nanoparticles	Hydrothermal Reduction	12
Ti-Cu	Closed Field Unbalanced Magnetron Sputtering (CFUBMS)	20
Au, Polycarbonate	Gamma radiation	21

[a] School of Materials Science and Engineering, University of Science and Technology Beijing, Beijing 100083, PR China. E-mail:383064167@qq.com; 18813120584@163.com, hangianyu@163.com; 1805246283@qq.com; ustblhy@163.com.
[b] School of Chemistry and Biological Engineering, University of Science and Technology Beijing, Beijing 100083, PR China. E-mail: zhouyabin_zyb@163.com
*Correspondence Address: University of Science and Technology Beijing, School of Material Science and Engineering Beijing, China. E-mail: zhengyudong@mater.ustb.edu.cn. Tel: +86-010-62330802
† Electronic Supplementary Information (ESI) available: The .ESI contains See DOI: 10.1039/x0xx00000x
‡ Ning Yan and Yabin Zhou have equally contributed as first authors.

	assisted diffusion	
Magnetic graphene oxide–TiO2 (MGO–TiO2)	Ultrasonic mix	22
ZnO films	Spray pyrolysis	23
Ag nanoparticles, mesoporous sintered activated carbon	Glucose reduction	24

One of the recently reported bio-based nanostructure carbon aerogels called pyrolysis BC (p-BC) aerogel has also caused great repercussions[25]. Its unique nanostructure and pore size distribution property makes it a suitable candidate for flexible solid-state energy storage device, oil/water separation, catalyst supports, sensors and so forth[26-28]. In addition, researchers use different materials to combine p-BC to improve its structure and electrical properties, thus expanding the application in the energy, acoustics and environmental fields[29-34]. Moreover, we think the "green" bio-based carbon materials with 3D nano-network structure should have better biological compatibility and match with tissues. But until now we found no literature reported on its biomedical applications.

Herein, we report a new convenient low-cost method to fabricate AgNP-deposited bio-based nanostructure carbon aerogels with an excellent antimicrobial properties, strong reabsorption of water ,and good mechanical properties. Then, it is followed by carbonization in nitrogen gas atmosphere. The synthesis process and structure of AgNP-BC were investigated by XRD (X-ray diffractometer), SEM (scanning electron microscopy), contact angles as well as EDS (energy dispersive spectrometer) tests. *In vitro* Ag releasing properties of p-BC/AgNP, water holding capacities and rehydration ability were measured in PBS buffer solution. Resilience was measured in air and PBS buffer solution respectively. The antibacterial activities of p-BC/AgNP against *E.coli* and *S.aureus* were demonstrated by disk diffusion and shake flask test method. Effects of p-BC/AgNP on cell growth were investigated through cultivation of Bel-7402 cells.

2. Materials and methods

2.1 Chemicals and materials

Bacterial cellulose membrane was offered by Hainan Yida Food Co. Ltd. (China). Silver nitrate ($AgNO_3$) and sodium hydroxide (NaOH) were purchased from Sinopharm Chemical Reagent Beijing Co. Ltd. Diamine Tetraacetic Acid (EDTA), Ethylene Tetrazolium Bromide (3-(4,5-dimethyl-2-thiazolyl)-2,5-diphenyl-2H, MTT) and trypsin were offered by Merck. Dulbecco's modified eagle medium (DMEM) was purchased from Gibcobrl. Other reagents and solvents were purchased from the domestic suppliers and used as received.

2.2 Preparation of BC/AgNP and p-BC/ AgNP

The BC/AgNP membrane was synthesized with an in-situ hydrothermal method according to our recent report[35]. The bacterial cellulose membranes were washed with deionized water and then immersed in 0.1 M NaOH solution at 95 ℃ for 1 h to remove the impurities. Then silver ammonia solution (Tollens reagent, 0.05M) was prepared. The purified BC membranes were soaked in silver ammonia solution for 24 h and then thoroughly washed to remove residual chemicals on surface. Subsequently, BC membranes were kept in a warm water bath at 95 ℃ for 30 min. BC/AgNP hybrid gel-membranes were obtained.

The membranes of BC and BC/AgNP were cut into rectangular or cubic shape with a sharp blade, frozen by liquid nitrogen (-196℃), and dried in a freeze dryer (Labconco Corporation, USA). After sublimation of ice, BC and BC/AgNP aerogels were generated. The obtained BC and BC/AgNP aerogels were transferred into a tubular furnace for carbonization under a nitrogen flow. The BC and BC/AgNP precursors were first heated at a heating rate of 2℃/min to 500℃, which temperature was kept for 1 h, then heated at 3℃/min to 800℃, which temperature was held for 2 h to allow complete pyrolysis, and third cooled at 5℃/min to 500℃, finally, naturally cooled to room temperature to yield black and ultralight aerogels. p-BC and p-BC/AgNP respectively representatives BC and BC/AgNP after carbonization.

2.3 Physical characterization

The microstructure of BC、BC/AgNP、p-BC and p-BC/AgNP were observed by SEM (Apollo 300, and 10 KV). All of the samples were freeze-dried and then coated with a thin layer of gold through a sputter coater in advance. Elemental maps of the AgNPs in p-BC/AgNP were obtained using EDS (Oxford).

CA (Contact angles) of p-BC and p-BC/AgNP were measured with an optical contact angle meter (OCA20, Dataphysics Inc) at ambient temperature. Water drop volumes were 3μl. PBS.

The phase identification and crystalline structure of BC、BC/AgNP、p-BC and p-BC/AgNP was studied by a Rigaku D/max-RB X-ray diffractometer (Rigaku Corporation, Japan). The samples were scanned from 10° to 70° at the speed of 10° /min. The data were processed using MDI/JADE6.0 software package.

The compressive tests of p-BC and p-BC/AgNP in air and PBS were performed by using an TA.XT Plus Texture Analyzer equipped with two flat-surface compression stages and 500 N load cells at 25℃.

2.4 Water holding capacity and reabsorption ability

The water holding capacities of BC、BC/AgNP、p-BC and p-BC/AgNP samples were determined gravimetrically after immersing these samples into PBS at 25℃. The samples were removed from water after 0.5 h, 1 h, 2 h, 4 h, 8 h, 12 h and 24 h, then weighed after removing the surface water. The water absorption capacity was calculated as

$$W_A = (M_t - M_0)/M_0 \quad (1)$$

in which W_t is the sample weight at time (0.5h, 1 h, 2h, 4 h, 8 h, 12h and 24 h), and W_0 is the sample dried weight.

For the measurement of the reabsorption ability, the absorbed samples BC, BC/AgNP, p-BC and p-BC/AgNP were compressed, with excess water absorbed by filter paper, and then put into the incubator (60℃). After 24 h, the dried samples were weighed noted as M1 and immersed into PBS again at 25℃. The samples' weight after absorbing water again after 24 h was noted as M_r. The reabsorption rate was calculated as

$$W_R = (M_r\text{-}M_1)/M_1 \quad (2)$$

At least three samples were performed for each measurement.

2.5 Release of silver *in vitro*

The kinetics of silver release was studied from the prepared BC/AgNP and p-BC/AgNP samples. BC/AgNP and p-BC/AgNP were cut into squares with side length of 15 mm. These samples were then immersed in 50 mL phosphate buffered saline (PBS, pH = 7.4) at 37 ℃. 5 mL solution was taken at regular time intervals (0.5 h, 1 h, 2 h, 3 h, 6 h, 12 h, 24 h, 36 h, 48 h and 72 h) from the remaining liquid , and 5 ml concentrated nitric acid was added to the solution to turn silver into silver ions completely and the amount of Ag released was analyzed using flame atomic absorption spectrophotometry (FAAS).

2.6 Antibacterial tests

The antibacterial activity was assessed by Gram-negative *Escherichia coli* (*E. coli*, ATCC 25922) and Gram-positive *Staphylococcus aureus* (*S. aureus*, ATCC 25923). *S. aureus* and *E. coli* were cultured on Luria-bertani (LB) agar plates. Two methods, the zone of inhibition and dynamic shake flask method, were adopted to evaluate the antibacterial activity according to our previous work[12]. The test specimens pure BC and BC/AgNP were cut into a disk shape with 6 mm diameter. p-BC and p-BC/AgNP were performed by disk diffusion assay, placed a 6 mm disk saturated with p-BC or p-BC/AgNP composite patch(with the same amount of BC and BC/AgNP) onto an agar plate[36]. All samples are required to be sterilized by autoclaving for 20 min at 121 ℃

For the the zone of inhibition, before culturing in an incubator at 37 ℃ for 24 h, samples were pressed into intimate contact with an agar culture medium inoculated with the *E.coli* and *S.aureus*. Subsequently, the zone of bacterial inhibition was monitored.

In the shake flask test method, 60 μ L suspension contained the bacteria was dropped onto the samples. After culturing for 24 h at 37 ℃, then wash the samples with the suspension and put into sterilized centrifugal tube with 1 mL LB culture solution. The tube was vigorously shaken for 30 s to detach the bacteria form the sample surface. Subsequently, the detached bacteria suspension was diluted 10 times. 2 mL of the diluted bacteria suspension was introduced onto the LB plates. Negative control samples were the blank LB plates in which 5 mL suspension of the bacteria inoculum and 5 mL of 0.9 % physiological saline were uniformly distributed. After culturing for 24 h at 37 ℃, the active bacteria was counted according to the National Standard of China GB/T 4789.2 protocol. The bacteriostatic rate was determined using the following formu

$$B_r\,(\text{Bacteriostatic rate}) = \frac{B-A}{B} \times 100\% \quad (2$$

where A, colony forming unit counts/mL (CFU/mL) of the negative control samples at 24 h; B, CFU/mL of the prepared samples at 24 h.

2.7 Cell culture

Bel-7402 cells were purchased from Shanghai Institutes for Biological Sciences (Shanghai, China). The cell lines were cultured in DMEM medium (Hyclone, Thermo Scientific, San Jose, CA) supplemented with 10 % fetal bovine serum (FBS; Hangzhou Sijiqing Biological Engineering Materials Co., Ltd., Hangzhou, China) solution. The cell lines were cultured in 10 cm plates, subcultured three times a week, and incubated in a humidity-controlled CO_2 incubator at 37 ℃ with 5 % CO_2.

Bel-7402 cells were used to investigate the morphology after carbonization with BC and BC/AgNP. The cell line Bel-7402 being used in experiments was a kind of malignant HCC cell with a high growth rate and great ability to excrete AFP[37], and it was frequently used as the model to study the cytotoxicity of samples[38, 39], to evaluate cell adhesion spreading and proliferation[40].In the *in vitro* experiment, Bel-7402 cells were cultured in 96-well plates for 12 h. Subsequently, suspension of BC and BC/AgNP, p-BC and p-BC/AgNP powder at concentrations of 0.05, 0.1 and 0.2 mg/mL was placed in 96-well plates containing the cells. After 24 h, the cell morphology was observed using an optical microscope (Life Technologies, Eugene, OR, USA). Meanwhile, after 1, 3 and 7 days, the cells were washed with PBS and fixed in 2 % paraformaldehyde for 30 min, and then permeabilized with 0.1 Triton-X 100 in PBS for 30 min. Nuclei were stained by incubating the cells with DAPI (1 mg/mL) and examined under an fluorescence microscope(Life Technologies, Eugene, OR, USA).

Cell viability was tested by MTT assays with different concentration of samples after 24 h, 48 h and 72 h. Briefly, 100 μ L of MTT (5 mg/mL) was added into each well followed by different time incubation at 37 ℃ in 5 % CO_2 incubator. Subsequently, the medium was removed carefully and 150 μ L of dimethyl sulfoxide (DMSO) was added to dissolve the formazan formed previously. Absorbance was recorded at 570 nm with a microtiter plate reader (Tecan Sunrise, Tecan Group AG, Zürich, Switzerland). Cells cultured with medium alone were used as control and the cell viability was considered as 100 %.

After one day's incubation of Bel-7402 cells with samples on cover glass, the cells were washed with PBS, fixed with 2.5 % glutaraldehyde at 4 ℃ for 30 min, and washed again with PBS. Next, cells were soaked in osmium tetroxide and washed with PBS. Then the cells were dehydrated by using an ethanol gradient (50 %, 75 %, 90 %, 95 % and 100 %) and dried in vacuum drying oven. Finally, the cells were coated with gold and observed by SEM.

2.8 Statistical analyses

Statistical analysis of data was performed by one-way analysis of variance (ANOVA), assuming confidence level of 95 % ($p < 0.05$) for statistical significance. All the data were expressed as means ± standard deviation (SD).

3. Results and discussion

3.1 Structure of p-BC/AgNP

The general strategy for fabricating AgNP deposited nano-structural carbon aerogels by in situ reduction and carbonization is illustrated in Fig 1A. Ag nanoparticles can be easily formed in situ in the interspace of the nanoscale BC fibers and various groups on fibers were decomposed in the pyrolysis process and turned into more "green" fibers (no harmful functional groups). Therefore, it is very easy and meaningful to produce AgNP-deposited carbon aerogels. To prevent the collapse of the network of BC, a freeze-drying technique was used to remove the water from BC and BC/AgNP to form a porous cellulose nanofibers aerogel (Fig.1B left). The dried aerogel was then pyrolyzed under flowing nitrogen gas at 800 ℃ to generate a black, ultralight and flexibility aerogel (Fig.1B right).

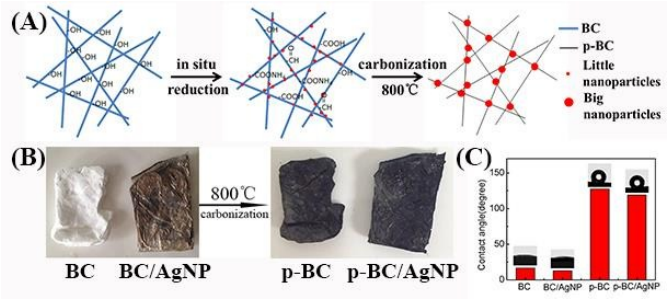

Fig.1. (A) Schematic representation of the fabrication process of AgNP deposited carbon aerogels by in situ reduction and carbonization; (B) The macro photograph of BC, BC/AgNP, p-BC and p-BC/AgNP; (C) Contact angles (CA) of BC, BC/AgNP, p-BC and p-BC/AgNP.

The SEM images in Fig. 2 show the morphologies of the BC、BC/AgNP、p-BC and p-BC/AgNP, respectively. BC aerogels have a porous, interconnected well-organized 3D network structure, which was formed through self-assembly in the bacteria culture process (Figure 2 A). High-magnification SEM image indicates that the nanofibers with a diameter of 20-80 nm are highly interconnected with large numbers of junctions (Figure 2 B). After the carbonization treatment, the porous 3D structure of BC aerogels maintained intact, but the diameter of the nanofibers decreased to 10–50 nm and some nanofibers were broken (Figure 2 E, F), due to the carbonization of the BC and evaporation of volatile species such as CO, CO_2, methanol, and acetic acid during pyrolysis[44]. Compared to pure nanofibers, BC loaded AgNPs possessed a 3D network with uniform silver nanoparticles evenly distributed. The granularity analysis (by image-pro plus 6.0) results showed that the particle diameters of more than 80% silver nano particles generated on BC nanofibers were in the range of 20-40 nm (the inset image in Fig. 2C). However, most particles' size of p-BC/AgNP were doubled, in which the average diameter of particles was about 80 nm (the inset image in Fig. 2G). This is mainly due to the heating process, the high energy of the nanoparticles aggregated in order to reduce the free enthalpy. However, due to obstruction of the BC network, most nanoparticles are not fully aggregated. In addition, silver particles were not departed or shed from nanofibers after pyrolysis. In contrast, they were evenly distributed and anchored on the fibers, and the nanofibers still maintained the original excellent 3D network structure (the image in Fig. 2 C, And EDS-analysis of p-BC/AgNP further confirmed the existence of silver in BC (Fig. 2I). Although there was O element in EDS spectrum, silver oxides did not occur in XRD.

The XRD patterns of pure BC, BC/AgNP, p-BC and p-BC/AgNP are shown in Fig. 2 J. The peaks at 2θ=14.7°, 16.8°and 23.2°of the BC sample could be attributed to the characteristic diffraction peaks of (110), ($1\ \overline{1}\ 0$) and (200) lattice plane of BC structure，respectively[45, 46]. The peak at 2θ=26.2° of the p-BC sample could be attributed to the characteristic diffraction peak of (002) lattice plane of Graphite. This diffraction peak belongs to the typical characteristic peaks of carbon material and reflects the degree of graphitization[25]. In the pattern of BC/AgNP and p-BC/AgNP, there has been some strong diffraction peaks located at 2θ=38.1°, 44.3°, 64.4°, 77.5°and 81.5°corresponded to the (111), (200), (220), (311) and (222) planes of Ag crystals, respectively[47, 48]. No characteristic diffraction peaks of Ag_2O, AgO, AgCl or other silver oxides appear in the pattern. On the basis of the results of XRD characterization, it also indicates that BC/AgNP and p-BC/AgNP were successfully prepared by previous methods. The average size of Ag particles is 26.24 and 74.76 nm, respectively, calculated from the (111) plane diffraction peak of Ag crystal by the Scherrer equation[49], identifying with the SEM results.

It was reported that many novel carbon aerogels had high compressive properties than the traditional aerogels[27]. Herein, the compressive stress-strain diagram of p-BC and p-BC/AgNP was investigated in Fig 3 A-D.

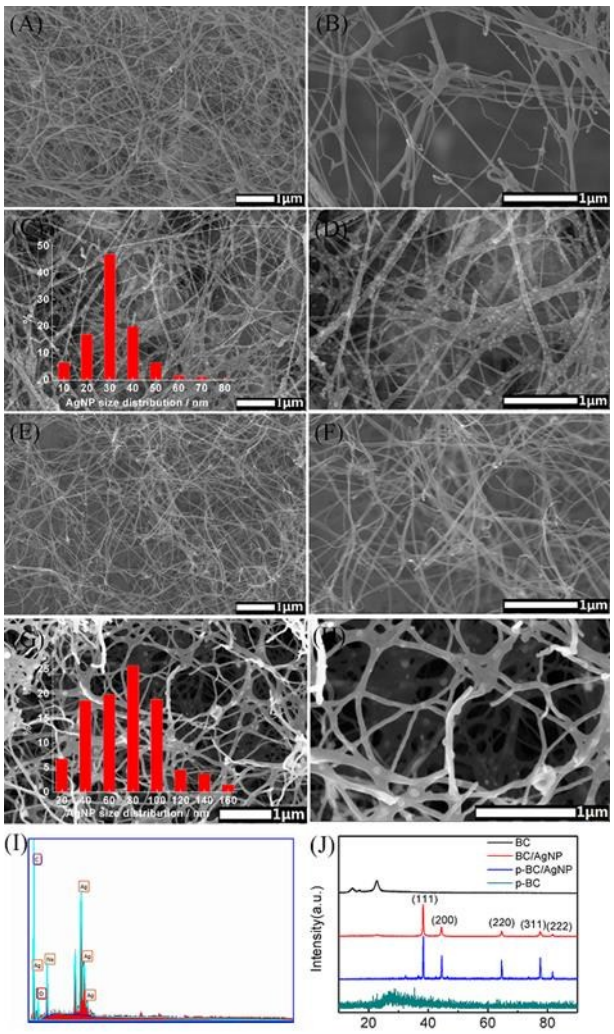

Fig. 2 SEM images of (A,B) pure BC, (C,D) BC/AgNP, (E,F) p-BC, (G,H) p-BC/AgNP, (I) EDS analysis of p-BC/AgNP and (J) XRD of BC, BC/AgNP, p-BC and p-BC/AgNP.

The p-BC aerogels can be compressed without crush after being subjected to a maximum strain of 90 % with a compressive strength of 30.7 kPa (Figure 3A) after one compression cycle. When the compressive load was removed, the p-BC aerogel returned to its original shape because of its unique interconnecting 3D network structures and elimination of the hydrogen-bond interaction in BC after pyrolysis. In contrast, after the compressive load was removed, BC aerogels did not return to its original shape because of the strongly interacting surface hydroxyl groups in the BC nanofibers[27]. Similar to p-BC, the p-BC/AgNP aerogel was almost completely recovered to its original volume when the compression was released (Figure 3B) and showed a relatively lower elastic compressibility, although it had a much lower compressive strength of 15.18 kPa at 90 % strain, most likely due to inhibition of Ag nanoparticles deposited on the carbonized fibers. The p-BC and p-BC/AgNP aerogels were subjected to a fatigue cyclic compression test (ε=90 %) by undergoing 100 loading/unloading cycles (Figure 3A, B). The unloading curves showed that the compressive stresses remained above zero until ε=0, suggesting almost complete recovery of the compressed aerogel after the cycle tests. During 100 compression cycles in air to 90 % strain , p-BC and p-BC/AgNP showed relatively minor decrease in the stress for the same strain level.

Remarkably, p-BC and p-BC/AgNP also can reversibly undergo large-strain deformation (up to 90 %) in liquids (such as PBS) (Fig. 3C, D). When liquid was reabsorbed during aerogel elongation, the measured stress exhibits some dependence on strain rate for strains between 80 % and 90 %. Furthermore, the measured stress for an aerogel containing PBS dips below zero for high axial-direction strains. These below-zero measured stresses result from the inability of liquid absorption to keep up with the giant true strain rate. The aerogels therefore adheres to the platens of the stress-strain measuring apparatus, causing the expected compressive stress temporarily switching to a tensile stress[50]. It can be seen that p-BC/AgNP has relatively nice compression elasticity both in air and liquid condition, which will expand its scope of application in multiple environments.

3.2 Water holding capacity and rehydration ability

As is well known, BC and BC/AgNP are excellent hydrophilic materials. Even though the dried BC aerogel or the product of freeze-dried BC hydrogel are super hydrophilic, their contact angles of water were close to 10° . In contrast, the p-BC and p-BC/AgNP became hydrophobic after carbonization, and the contact angles of them were 127.5° and 119.1° , respectively (Figure 1C).

Although some materials were hydrophobic, they can still absorb a lot of water due to porous structure in a certain period of time[51]. The water absorption capacities of BC, BC/AgNP, p-BC and p-BC/AgNP were monitored for a period of 24h after samples were immersed in PBS at 37 ℃. As shown in Fig. 5 A, after 1 hour's immersion, the water sorption ratio was equal to 24.5, 19.8, 11.6 and 8.9, for BC, BC/AgNP, p-BC and p-BC/AgNP, respectively. As expected, the high porosity and large numbers of hydrophilic groups of aerogels led to a faster initial water sorption rate after just 1 h (for BC and BC/AgNP)[52]. Simultaneously, the water absorption ratio reached its maximum in a short time. After 24 h of immersion, all the samples were already significantly immersed in water and reached its maximum water sorption capacity. While in the process of water absorption, BC and BC/AgNP showed a high liquid water absorption rate which was probably due to its porous structure and large numbers of hydrogen bonds, and the maximum water absorption capacities were 28.7 and 27.7 respectively; p-BC and p-BC/AgNP showed a slow absorption rate and ultimately achieved a relatively high water absorption capacities of 26.5 and 25.3, respectively. The slow water absorption rate of p-BC and p-BC/AgNP is attributed to the hydrophobic material itself, but with its unique three-dimensional network porous structure, the water molecules will be pushed into the pores as time passed, and finally achieve a relatively high water absorption capacity.

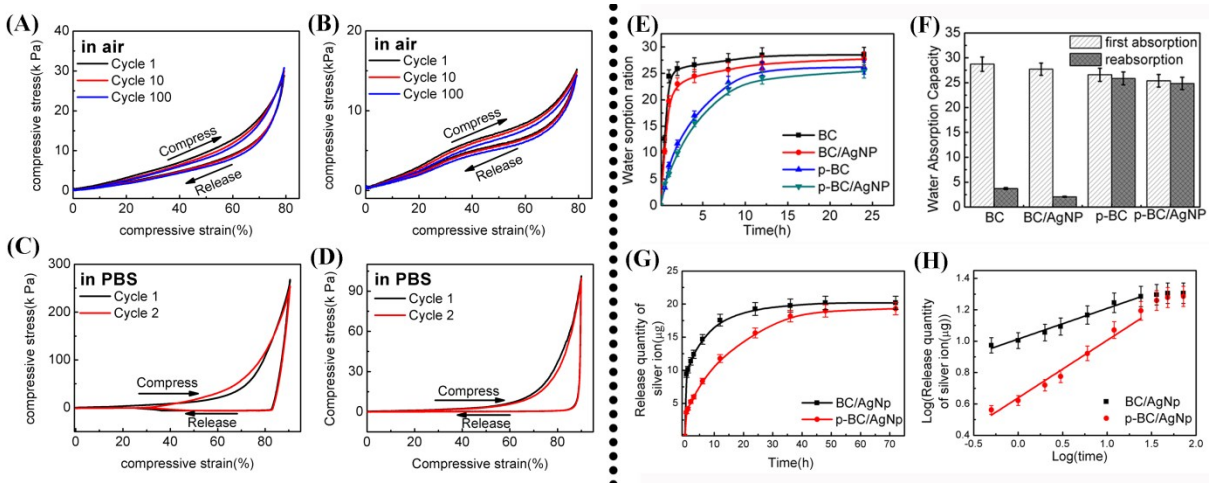

Fig. 3 The compressive stress to reach 90 % strain of p-BC (A) and p-BC/AgNP (B) at an engineering strain rate of 1 mm /s-1 is plotted as a function of cycle number for 100 cycles in air; Mechanical property measurements as PBS is pushed out and sucked in during 90 % compressive stroke for p-BC (C) and p-BC/AgNP (D); (E) Water sorption ratio of BC, BC /AgNP, p-BC and p-BC/AgNP after 0.5h, 1 h, 2h, 4 h, 8h, 12h and 24 h of immersion in PBS (at 25 ℃); (F) Reabsorption rate of BC, BC /AgNP, p-BC and p-BC/AgNP. (G) Release quantity changes of silver ion in PBS buffer solution;(H) log(release quantity of Ag+) vs log(times) curve.

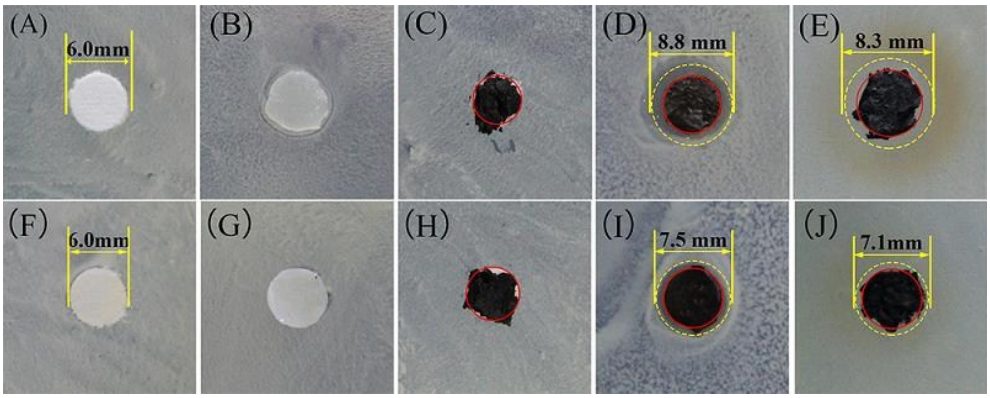

Fig. 4 The inhibition zone test for E. coli (A-E) and S. aureus (F-J) of blank (A and F), BC (B and G), p-BC (C and H), BC /AgNP (D and I)and p-BC/AgNP (E and J).

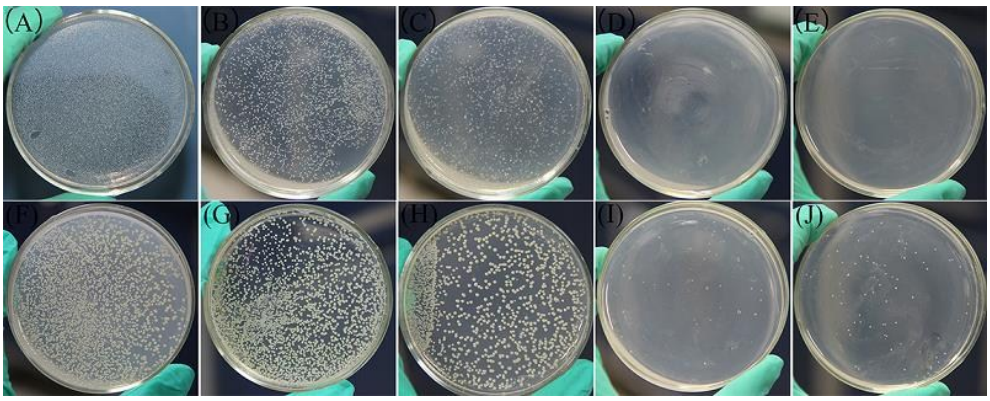

Fig. 5 Re-cultivated bacterial colonies after 24 h on agar: E. coli (A-E) and S. aureus (F-J) colonies are previously dissociated from blank (A and F), BC (B and G), p-BC (C and H), BC /AgNP (D and I) and p-BC/AgNP (E and J).The S. aureus and E. coli bacteria concentration seeded on the samples is 104 cfu/mL.

For water reabsorption capacity, the original three-dimensional network structure and the hydrogen bond of hydrous BC would be destroyed after drying and deformation, so that the entire 3D-network structure after drying was destroyed and difficult to recover before absorption, therefore BC and BC/AgNP have a low rehydration rate(Fig. 3F), in which the rehydration rates were 3.72 and 2.06, respectively. On the contrary, p-BC and p-BC/AgNP have a very good compression elasticity after carbonization, both of them could substantially restore the original shape after drying and deformation, and have a high rehydration rate of 25.84 and 24.83, respectively, which showed a slight decrease compared to first water absorption. After absorbing PBS again, the reabsorption capacity of p-BC/AgNP and p-BC was obviously higher than BC/AgNP and BC. Accordingly, carbonized p-BC and p-BC/AgNP have greater advantages on absorbent and rehydration over BC and BC/AgNP, so p-BC/AgNP will have a prospect on the relevant medical fields, such as wound dressing and drug release carrier fields.

3.3 Release of silver *in vitro*

Silver nanoparticles have excellent antibacterial properties[12], but it may shed from materials and then enter the human body, bringing some hazards. The release quantity and rate of silver ions play an important role in their antibacterial effect and biological safety. The silver content of samples obtained by FAAS was 0.148mg. Ag^+ releasing profiles of BC/AgNP and p-BC/AgNP in PBS solution were depicted by kinetics curve and logarithmic fitting curve in the Fig.3 G and H, respectively. The Ag^+ releasing kinetics curve of samples followed an logarithmic increase with the release time, which depending on combination of silver with fiber and hydrophilicity or hydrophobicity of the matrix material. The release rate of Ag^+ is proportional to tn at first, and after several hours, the release rate tends to equilibrium. Moreover, the value of n varied for different samples which is indicative of different transport mechanisms[53, 54]. The logarithmic fitting curve showed the power law exponent for Ag^+ release of p-BC/AgNP is 0.36 with R^2 = 0.96, indicating the relatively high static correlation between the exponential power law and experimental measurements. The power law exponent of BC/AgNP is 0.19, with R^2 of fitting coefficient 0.97, which may be attributed to better hydrophilic of BC, and nano silver can diffuse into the solution in a short time. Furthermore, after six hours, the Ag^+ releasing amount of BC/AgNP has a violent process, while it requires double time for p-BC/AgNP to release the same amount of Ag+, the binding force of BC was worse than p-BC/AgNP. However, after 48 hours, the release amount of BC/AgNP and p-BC/AgNP reached a stable value and the maximum, 20.19 μg and 19.31 μg, respectively. Therefore, compared with BC/AgNP, p-BC/AgNP has a relatively stable and slow rate of release of silver ions, and also can basically reach the release rate levels of BC/AgNP. In summary, p-BC/AgNP has a more stable and long-lasting anti-bacterial properties, and can further be used in various fields of biological, medical, health, etc.

3.4 Antibacterial properties

The antibacterial activities of BC、BC/AgNP、p-BC and p-BC/AgNP against E.coli and S.aureus, which are all common bacteria of infection, were measured by the disk diffusion method after 24 h incubation at 37 ℃(Figure.4 A~J). As expected, the normal growth of E.coli and S.aureus was seen in the agar plate when nothing was introduced. The blank control with only filter paper demonstrated almost no antibacterial activity without the addition of Ag nanoparticles (Fig. 4A, F), and no inhibition zone was observed for the pure BC and p-BC as control (Fig. 4B, D, G, I). In contrast, the diameters of inhibition zone from BC/AgNP and p-BC/AgNP on E. coli/S. aureus were 8.8/7.5 mm and 8.3/7.1 mm, respectively.

Table 2 The antibacterial quantitative data of BC,BC /AgNP, p-BC and p-BC/AgNP (A) *E. coli* (B) *S.aureus*

(A)	Negative control ($\times 10^4$)	BC ($\times 10^4$)	p-BC ($\times 10^4$)	BC/AgNP	p-BC/AgNP
Colonies after 24h/cfu	3.2	2.6	2.0	0	0
B_r		—	—	100%	100%
(B)	Negative control ($\times 10^4$)	BC ($\times 10^4$)	p-BC ($\times 10^4$)	BC/AgNP	p-BC/AgNP
Colonies after 24h/cfu	2.8	2.6	2.1	62	82
B_r		—	—	99.8%	99.7%

In order to acquire more information about antibacterial activity of samples for quantitative analysis, the antibacterial rates of four samples against E. coli and S. aureus were tested by the shake flask test method (Fig. 5). As the previous results of inhibition zone, after 24 h of incubation, the ratio of bacterial (both E. coli and S. aureus) growth of blank group, BC and p-BC groups were in same order of magnitude, and bactericidal rate (Br) of BC/AgNP and p-BC/AgNP groups were 99.7%~100% (Table 2). The results showed that the antimicrobial effects of p-BC/AgNP were similar to the antimicrobial effects of the BC/AgNP, and existing literatures12 have shown that antimicrobial effects of BC/AgNP could be comparable with commercial silver-containing dressings. At the same time, compared with the traditional silver-dispersed carbon aerogels antibacterial materials[55], the preparation of bio-based carbon aerogel is more environmentally friendly and easy, in addition, fewer silver content of p-BC/AgNP also has a good antibacterial property. So, p-BC/AgNP can be used as an excellent antimicrobial material.

3.5 Cytocompatibility

The biocompatibility of BC、BC/AgNP、p-BC and p-BC/AgNP was evaluated by co-culturing with Bel-7402 cells after 1, 3 and 7 days. Cell proliferations and morphologic changes are shown in ESI, Fig 1. Optical microscope (OM) observations at 200× revealed that, after 24h, the cells of the control group had a large amount of squamous Bel-7402 cells that were adherent, evenly distributed and formed a monolayer, and those of the experimental groups also had an excellent cell viability after 24 h.

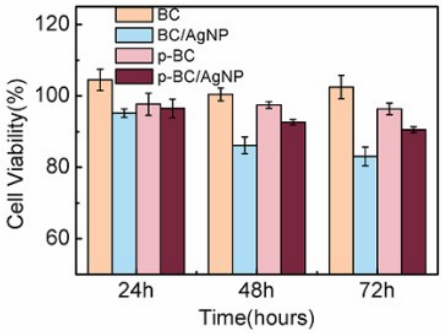

Fig. 6 Time-dependent viability of Bel-7402 cells treated with BC, BC/AgNP, p-BC and p-BC/AgNP(0.2 mg/mL). * $p < 0.05$ compared to control.

MTT assays were also performed to assess the cytotoxicity of samples in this study (Fig. 6). Bel-7402 cells were cultured in medium (0.2 mg/mL) with four samples to confirm the biocompatibility between the cells and experimental materials. After 24 h, though the BC sample exhibited slightly higher MTT absorbance results than the other three samples, there were no obvious differences between BC and BC/AgNP, p-BC or p-BC/AgNP, in which the cell survival rates were all more than 90 % (compared to the control, $p < 0.05$), as determined by MTT. With increasing culture time, the viability of cells on each sample shows significant difference. The cell viability of BC and p-BC with no silver were all more than 90 %, and the ratio of BC was higher, mainly due to the BC was natural product, and it can provide nutrition to cells. In contrast, the cell viability of BC/AgNP and p-BC/AgNP had significantly lower silver than BC and p-BC. What's more, the MTT data of BC/AgNP was less than 90 %, while the p-BC/AgNP group was more than 90 %. With the time passed, the cell activity of p-BC/AgNP was obviously higher than BC/AgNP. This proves that the cytotoxicity of p-BC/AgNP is markedly lower than BC/AgNP, and pyrolysis is absolutely necessary to make it more biocompatible.

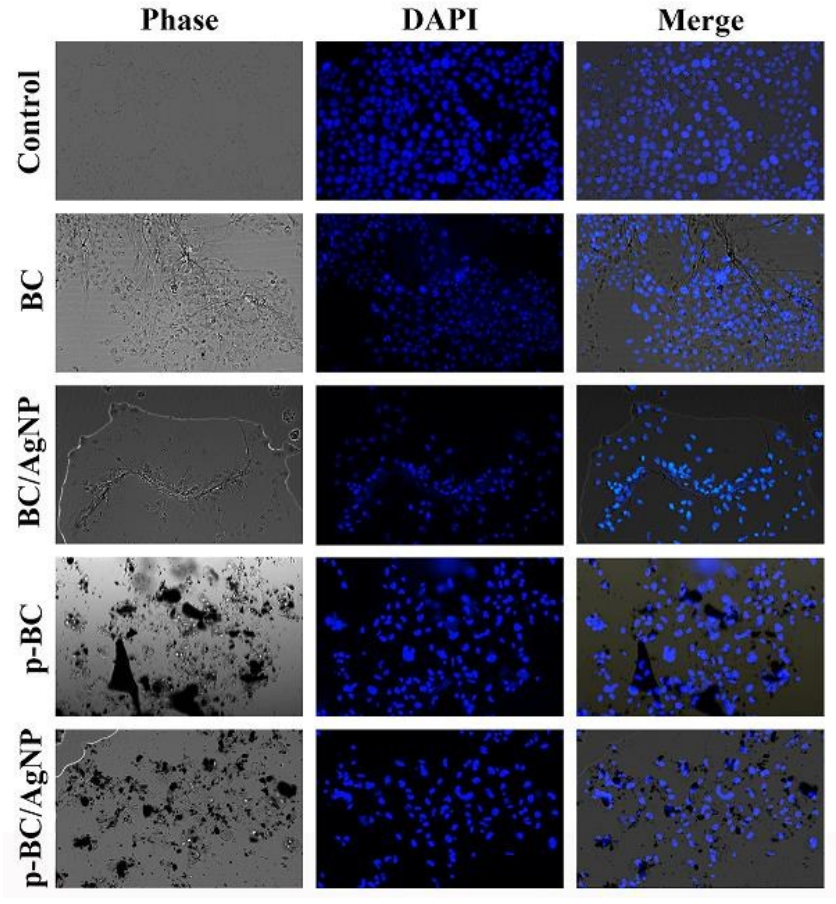

Fig. 7 Analysis of the effect of four samples on apoptosis in Bel-7402 cells. After 7days, samples (0.1 mg/mL) cultured in DMEM medium were collected and subjected to DAPI staining (blue), they showed intact nuclei (Optical microscope (OM):first row ; fluorescence optical microscope (FOM): second row).

DAPI fluorescence staining also used to further assess the effect of samples on the Bel-7402 cells. The Bel-7402 cells were cultured with samples suspension (0.1 mg/mL) for 7 day. Then, the DAPI fluorescence staining was used to further confirm the relationship between samples and cells. This method can allow the observation of cell apoptosis induced by samples. Fig. 7 (second row) shows the DAPI-stained of intact nuclei of Bel-7402 cells, as observed under a fluorescence optical microscope (FOM). This means that Bel-7402 cells cultured with different samples suspension for 7 days did not induce apoptosis and these samples showed good biocompatibility. By comparing the results of the 7th day of the picture merge by DAPI-stained (blue) and bright fields, after culturing for 1 day, Bel-7402 cells were sparsely spread more or less everywhere with tiny dense cell domains. Most Bel-7402 cells appeared in flat shape, and there were no significant differences between experimental groups. On the 4th day, the number of cells increased obviously, demonstrating that Bel-7402 cells proliferation had begun. After culturing for 7 days, more cells grew in all groups and then converged to form large areas in the vicinity of BC and BC/AgNP, as shown in Fig. 7. On the contrary, no cell groups appear around the p-BC and p-BC/AgNP, while large numbers of cells were relatively evenly distributed within the range of vision. This means that p-BC owns a good biocompatibility, like other carbon materials[41, 56].

The SEM high-resolution images also show the structure and quantity of cells after cultivating with samples. The cell morphologies of Bel-7402 on glass covering with BC and BC/AgNP, p-BC or p-BC/AgNP after 1 days of culture were shown in Figure 8 (A~I). One could see that Bel-7402 cells with all samples spread out and displayed a flattened phenotype and relatively uniform distribution. Viewing the magnified shape and structure of the cells, the images (Fig. 8 B, D, F, H and J) showed intact cell structure and spindle flat cell morphology, respectively. Simultaneously, the images also showed the structure of lamellipodium and filopodium. They were mainly made of actin filaments and helpful to maintain cellular environment before cells beginning to migrate[42]. In quantity of the cells, the cells number of BC/AgNP group was significantly less than other groups, consistent with the results of the MTT assay. Therefore, it can be concluded that the p-BC/AgNP improved the stability and had no cytotoxicity.

In vitro experimental results demonstrated p-BC/AgNP had relatively low cytotoxicity due to the “green” nano fibers and the slow releasing of Ag^{+}. This made it can be used on biomedical fields.

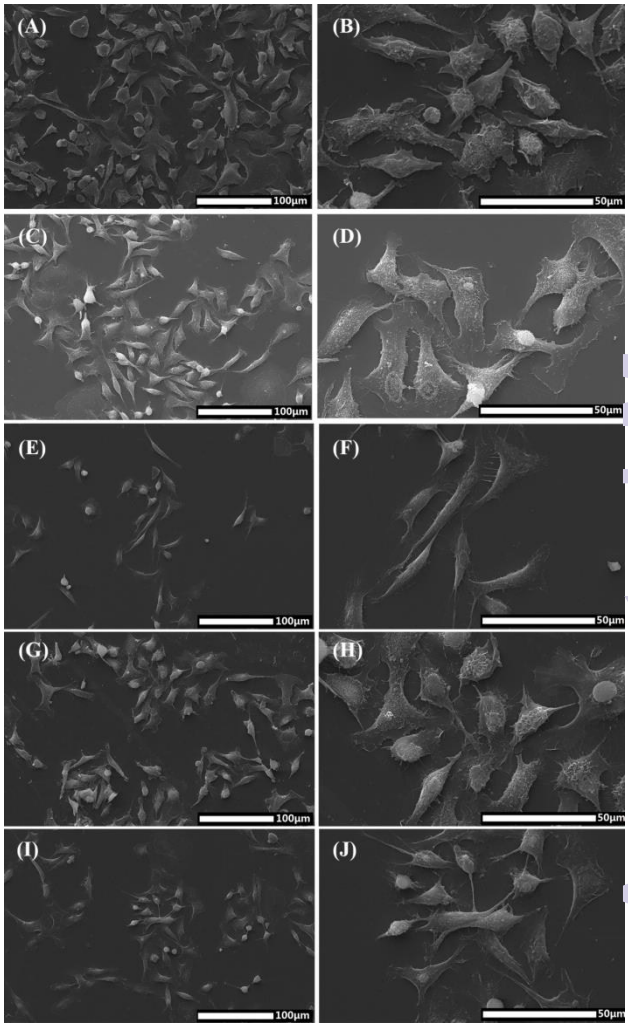

Fig. 8 Morphology of Bel-7402 cells cultured with BC (C,D), BC/AgNP (E,F), p-BC (G,H) and p-BC/AgNP (I,J) (0.1 mg/mL) and control (A,B) for 24 h was observed using SEM, normal morphology of cells and its large quantity showed the good biocompatibility of samples.

Conclusions

In this study, AgNP-deposited bio-based nanostructure carbon aerogels derived from BC/AgNP have been successfully fabricated in a method of in situ reaction and carbonization. The unique 3D nano-network structure and pore distribution gave p-BC/AgNP good compression elasticity in air and liquid condition. The excellent cellular network structure make the hydrophobic p-BC/AgNP aerogels having a nice reabsorption capacity, the rate reached to 24.83, far more than BC/AgNP. Moreover, compared to BC/AgNP, p-BC/AgNP has a slow release rate of silver, while its total amount of Ag release is

close to BC/AgNP after 48 h, due to the stronger combination of Ag and carbon nanofibers, thus avoiding the damage caused by high concentration of silver in short-term. Also p-BC/AgNP has excellent antibacterial effect on *E. coli* and *S. aureus*, in which the inhibition rate was over 99 %. In addition, p-BC/AgNP shows a good biocompatibility with Bel-7402 cells, the cells survival rate is more than 90 % and cells can differentiate and grow normally after a period of time. Therefore, p-BC/AgNP carbon aerogel might be a desirable antibacterial material that could be used as a new kind of wound dressing, implants , drug release carrier, and other biomedical fields.

Acknowledgements

This work is supported by National Natural Science Foundation of China (No.51273021, 51473019).

Notes and references

1. J. Li, X. Wang, Q. Huang, S. Gamboa and P. J. Sebastian, *Journal of Power Sources*, 2006, **158**, 784-788.
2. C. Moreno-Castilla and F. J. Maldonado-Hódar, *Carbon*, 2005, **43**, 455-465.
3. S. A. Waghuley, S. M. Yenorkar, S. S. Yawale and S. P. Yawale, *Sensors and Actuators B: Chemical*, 2008, **128**, 366-373.
4. S. Zhang, D. Wu, L. Wan, H. Tan and R. Fu, *Journal of Applied Polymer Science*, 2006, **102**, 1030-1037.
5. G. M. P. Alain C. Pierre, *Chemical Reviews*, 2002, **102**.
6. A. M. ElKhatat and S. A. Al-Muhtaseb, *Advanced Materials*, 2011, **23**, 2887-2903.
7. H. Bi, Z. Yin, X. Cao, X. Xie, C. Tan, X. Huang, B. Chen, F. Chen, Q. Yang, X. Bu, X. Lu, L. Sun and H. Zhang, *Advanced Materials*, 2013, **25**, 5916-5921.
8. H. Bi, X. Huang, X. Wu, X. Cao, C. Tan, Z. Yin, X. Lu, L. Sun and H. Zhang, *Small*, 2014, **10**, 3544-3550.
9. N. Shah, M. Ul-Islam, W. A. Khattak and J. K. Park, *Carbohydrate polymers*, 2013, **98**, 1585-1598.
10. F. G. Torres, S. Commeaux and O. P. Troncoso, *Journal of functional biomaterials*, 2012, **3**, 864-878.
11. L. Huang, X. Chen, T. X. Nguyen, H. Tang, L. Zhang and G. Yang, *Journal of Materials Chemistry B*, 2013, **1**, 2976.
12. J. Wu, Y. Zheng, W. Song, J. Luan, X. Wen, Z. Wu, X. Chen, Q. Wang and S. Guo, *Carbohydrate polymers*, 2014, **102**, 762-771.
13. D. Ciechanska, *Fibres and Textiles in Eastern Europe*, 2004, **12**.
14. K. Ghule, A. V. Ghule, B.-J. Chen and Y.-C. Ling, *Green Chemistry*, 2006, **8**, 1034.
15. J. Gutierrez, A. Tercjak, I. Algar, A. Retegi and I. Mondragon, *Journal of colloid and interface science*, 2012, **377**, 88-93.
16. M. Ul-Islam, T. Khan, W. A. Khattak and J. K. Park, *Cellulose*, 2012, **20**, 589-596.
17. A. R. Figueiredo, A. G. Figueiredo, N. H. Silva, A. Barros-Timmons, A. Almeida, A. J. Silvestre and C. S. Freire, *Carbohydrate polymers*, 2015, **123**, 443-453.
18. R. J. Pinto, P. A. Marques, C. P. Neto, T. Trindade, S. Daina and P. Sadocco, *Acta biomaterialia*, 2009, **5**, 2279-2289.
19. J. X. Guang Yang, Feng Hong, Zhangjun Cao, Xuexia Yang., *Carbohydrate Polymers*, 2012, **87**.
20. X. Jin, L. Gao, E. Liu, F. Yu, X. Shu and H. Wang, *Journal of the mechanical behavior of biomedical materials*, 2015, **50**, 23-32.
21. K. Hareesh, A. V. Deore, S. S. Dahiwale, G. Sanjeev, D. Kanjilal, S. Ojha, N. A. Dhole, K. M. Kodam, V. N. Bhoraskar and S. D. Dhole, *Radiation Physics and Chemistry*, 2015, **112**, 97-103.
22. Y.-N. Chang, X.-M. Ou, G.-M. Zeng, J.-L. Gong, C.-H. Deng, Y. Jiang, J. Liang, G.-Q. Yuan, H.-Y. Liu and X. He, *Applied Surface Science*, 2015, **343**, 1-10.
23. C. Manoharan, G. Pavithra, S. Dhanapandian and P. Dhamodharan, *Spectrochimica acta. Part A, Molecular and biomolecular spectroscopy*, 2015, **149**, 793-799.
24. W. Wang, K. Xiao, T. He and L. Zhu, *Journal of Alloys and Compounds*, 2015, **647**, 1007-1012.
25. Z. Wu, C. Li, H. Liang, J. Chen and S. Yu, *Angewandte Chemie International Edition*, 2013, **52**, 2925-2929.
26. E. H. Falk Liebner, Antje Potthast,Thomas Rosenau, *Cellulosic Aerogels*, Youssef Habibi, Lucian A. Lucia, 2012.
27. H. Liang, Q. Guan, Z. Zhu, L. Song, H. Yao, X. Lei and S. Yu, *NPG Asia Materials*, 2012, **4**, e19.
28. L. Chen, Z. Huang, H. Liang, W. Yao, Z. Yu and S. Yu, *Energy & Environmental Science*, 2013, **6**, 3331.
29. Z. Wang, Y. Ma, H. He, C. Pei and P. He, *Applied Surface Science*, 2015, **332**, 456-462.
30. B. Dai, X. Shao, Y. Ren, G. Wang, C. Pei and Y. Ma, *Materials Letters*, 2012, **82**, 188-190.
31. Y. Ren, S. Li, B. Dai and X. Huang, *Applied Surface Science*, 2014, **311**, 1-4.
32. C. Long, D. Qi, T. Wei, J. Yan, L. Jiang and Z. Fan, *Advanced Functional Materials*, 2014, **24**, 3953-3961.
33. W. Wang, Y. Sun, B. Liu, S. Wang and M. Cao, *Carbon*, 2015, **91**, 56-65.
34. Y. Huang, T. Wang, M. Ji, J. Yang, C. Zhu and D. Sun, *Materials Letters*, 2014, **128**, 93-96.
35. T. Zhang, Y. Zheng, S. Liu, L. Yue, Y. Gao and Y. Yao, *Journal of Electroanalytical Chemistry*, 2015, DOI: 10.1016/j.jelechem.2015.05.005.
36. S. Li, X. Yan, Z. Yang, Y. Yang, X. Liu and J. Zou, *Applied Surface Science*, 2014, **292**, 480-487.
37. B. Y. Wu, H. F. Wang, J. T. Chen and X. P. Yan, *Journal of the American Chemical Society*, 2011, **133**, 686-688.
38. Z. Hu, X. Fan, H. Wang and J. Wang, *Polymer*, 2009, **50**, 4175-4181.
39. S. P. Xin Zeng, Jie Li, Chi Wang, Yuting Wen, Hongmei Wu, Cuifeng Wang, Chuanbin Wu and Min Feng, *Nanotechnology*, 2011, **22**, 1-13.
40. H. J. Wang, J. X. Fu and J. Y. Wang, *Colloids and surfaces. B, Biointerfaces*, 2009, **69**, 109-115.
41. C. Karavasili, E. P. Amanatiadou, L. Sygellou, D. K. Giasafaki, T. A. Steriotis, G. C. Charalambopoulou, I. S. Vizirianakis and D. G. Fatouros, *Journal of Materials Chemistry B*, 2013, **1**, 3167.
42. M.-C. Hung, S.-Y. Yuan, S. I. Chang, J.-W. Liao, T.-H. Ko and C.-L. Cheng, *Carbon*, 2014, **68**, 628-637.
43. S. J. Cho, S. M. Jung, M. Kang, H. S. Shin and J. H. You, *Polymer*, 2015, **69**, 95-102.
44. Y. Wan, G. Zuo, F. Yu, Y. Huang, K. Ren and H. Luo, *Surface and Coatings Technology*, 2011, **205**, 2938-2946.

45. H. Luo, J. Zhang, G. Xiong and Y. Wan, *Carbohydrate polymers*, 2014, **111**, 722-728.
46. S. Y. Oh, D. I. Yoo, Y. Shin, H. C. Kim, H. Y. Kim, Y. S. Chung, W. H. Park and J. H. Youk, *Carbohydrate research*, 2005, **340**, 2376-2391.
47. S. Ristig, O. Prymak, K. Loza, M. Gocyla, W. Meyer-Zaika, M. Heggen, D. Raabe and M. Epple, *J. Mater. Chem. B*, 2015, DOI: 10.1039/c5tb00644a.
48. A. Mandal, S. Sekar, N. Chandrasekaran, A. Mukherjee and T. P. Sastry, *J. Mater. Chem. B*, 2015, **3**, 3032-3043.
49. C. K. Sathiya and S. Akilandeswari, *Spectrochimica acta. Part A, Molecular and biomolecular spectroscopy*, 2014, **128**, 337-341.
50. Y. Wu, N. Yi, L. Huang, T. Zhang, S. Fang, H. Chang, N. Li, J. Oh, J. A. Lee, M. Kozlov, A. C. Chipara, H. Terrones, P. Xiao, G. Long, Y. Huang, F. Zhang, L. Zhang, X. Lepro, C. Haines, M. D. Lima, N. P. Lopez, L. P. Rajukumar, A. L. Elias, S. Feng, S. J. Kim, N. T. Narayanan, P. M. Ajayan, M. Terrones, A. Aliev, P. Chu, Z. Zhang, R. H. Baughman and Y. Chen, *Nature communications*, 2015, **6**, 6141.
51. S. T. Nguyen, J. Feng, S. K. Ng, J. P. W. Wong, V. B. C. Tan and H. M. Duong, *Colloids and Surfaces A: Physicochemical and Engineering Aspects*, 2014, **445**, 128-134.
52. Y. Wang, S. Yadav, T. Heinlein, V. Konjik, H. Breitzke, G. Buntkowsky, J. J. Schneider and K. Zhang, *RSC Advances*, 2014, **4**, 21553.
53. D. R. Paul, *International journal of pharmaceutics*, 2011, **418**, 13-17.
54. J. Siepmann and N. A. Peppas, *International journal of pharmaceutics*, 2011, **418**, 6-12.
55. S. Zhang, R. Fu, D. Wu, W. Xu, Q. Ye and Z. Chen, *Carbon*, 2004, **42**, 3209-3216.
56. S. I. Kim, B. B. Sahu, S. E. Kim, A. Ali, E. H. Choi and J. G. Han, *J. Mater. Chem. B*, 2015, **3**, 3267-3278.

Graphical abstract

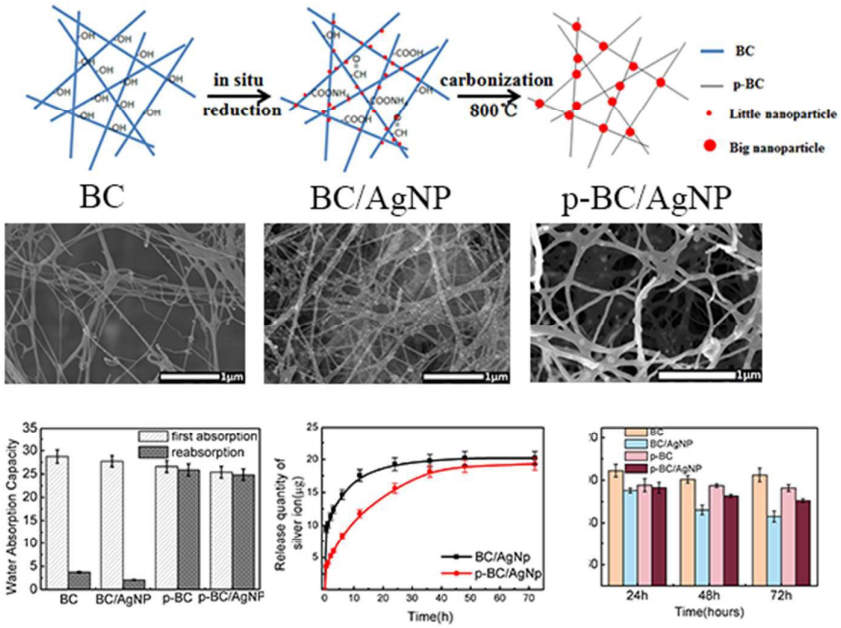

p-BC/AgNP carbon aerogel were prepared by in situ reduction and carbonization, which owned an excellent reabsorption capacity, mechanical properties, as well as better antibacterial behavior and biocompatibility due to the slow controllable release of silver from the three-dimensional network of p-BC/AgNP.